DC Powerline Communication System using a Transmission Line Transformer for High Degree of Freedom Applications

By

Eric R. Wade

B.S., Mechanical Engineering
Massachusetts Institute of Technology (2000)

Submitted to the Department of Mechanical Engineering and the
Department of Electrical Engineering and Computer Science
in Partial Fulfillment of the Requirements for the Degrees of

Master of Science in Mechanical Engineering
and
Master of Science in Electrical Engineering and Computer Science

at the
Massachusetts Institute of Technology
June 2004

Signature of Author .....
Department of Mechanical Engineering
May 7, 2004

Certified by .....
Haruhiko H. Asada
Professor of Mechanical Engineering
Thesis Supervisor

Accepted by .....
Ain A. Sonin
Chairman, Department Committee on Graduate Students
Department of Mechanical Engineering

Accepted by .....
Arthur C. Smith
Chairman, Department Committee on Graduate Students
Department of Electrical Engineering and Computer Science

DC Powerline Communication System using a Transmission Line Transformer for High Degree of Freedom Applications

by

Eric R. Wade

Submitted to the Department of Mechanical Engineering and the
Department of Electrical Engineering and Computer Science
on May 7, 2004 in partial fulfillment of the
requirements for the Degrees of Master of Science in
Mechanical Engineering
and of Master of Science in
Electrical Engineering and Computer Science

ABSTRACT

A new type of powerline communication is developed to reduce cable requirements for robotic, electromechanical, and vehicular systems. A DC power bus line connecting a DC power supply to motor drives and sensor units is used for transmitting both data and DC power. Unlike conventional AC powerline communication, the DC power bus provides amenable and predictable noise characteristics and desirable impedance characteristics that allow for large fanout and high bandwidth. First the basic architecture of DC powerline communication is presented, followed by verification of the feasibility of using a DC power bus as a communication medium. A high-fanout modem is then designed using a Guanella type transmission line transformer (TLT). The modem characteristics including high-frequency parasitic dynamics are analyzed, and the overall line impedance and signal attenuation are evaluated as the number of nodes goes to infinity. A prototype DC powerline communication system is then designed, built, and tested. The serial windings and special resonance characteristics of TLT coupled with a capacitor are exploited to minimize attenuation in high fanout systems. As a result the prototype modem can broadcast data to more than 100 nodes simultaneously.

Thesis Supervisor: Haruhiko H. Asada
Title: Professor of Mechanical Engineering

ACKNOWLEDGMENTS

I wish to thank my parents, Leslie and Jerome, and my brothers, Neil, Craig, and Jerome Jr., for their support throughout my academic endeavors. I wish to thank my fiancée, Mikii Williams, for her unfailing love and support. I wish also to thank Prof. Asada whose guidance, creativity, and patience all made this work possible. Finally, thanks to all of my lab mates who made the late nights and long hours a little more bearable.

TABLE OF CONTENTS

TABLE OF FIGURES

INTRODUCTION

The number of actuators and sensors used in robotic systems, automobiles, and manufacturing equipment keeps increasing. A humanoid robot, such as Honda's ASIMO, has 26 actuators and at least 6 sensors [1]. Current high-end automobiles have over 200 actuators and numerous sensors. A standard machining center contains more than 10 actuators and 50 sensors for work loading and miscellaneous functions in addition to four-to-six high precision servos. The design of a standard servoed axis entails two cables connecting the actuator to its driver and controller; one is a signal cable for the encoder and other sensors, and the other is a power cable for delivering high voltage/current power to the actuator. As the number of degrees-of-freedom (d.o.f.) increases, these cables create major problems: they are a bottleneck in design and fabrication, as well as an impediment for cost reduction, maintenance and reliability.

This cabling is a design limitation. Special consideration must be made for any node located through a bending or rotating joint to prevent arcing or fraying of the cables. Furthermore, power cable lines between an actuator and its drive amplifier create electromagnetic interference (EMI) and noise problems. Care must be taken in routing signal lines and power lines together. Additionally, cabling is extremely costly. For instance, in automobiles, reducing the total weight by a pound saves $3 - $6 [2]. Finally, cabling makes installation and maintenance difficult. The complex routing requirements often preclude automated installation, and the cables can obstruct maintenance efforts.

The industry has been striving to reduce cables. First, technology has been established for replacing serial data lines by a parallel line, thereby reducing the number of wires. Various standards have been established for such data lines, including those

described in [3]. Although these bus lines reduce the cable thickness, two separate cables are still required for signal and power transmissions in each servoed axis.

Powerline communication (PLC), on the other hand, consolidates these two lines by sending data over already existing power lines. It allows us to reduce cabling requirements, and has been shown to be a useful and economically viable technology in recent years [4][5]. The bulk of PLC research to this point has been done in regards to in-home networks. Current PLC techniques allow signal speeds of up to 1kbps and are expected to reach up to 1Mbps, and cover communication methods such as phase-locked loop, spread spectrum, and digital modulation techniques [5][6][7]. However, there are a number of limitations to PLC. The large power transformers that are used to step down power from outdoor power lines to individual houses attenuate high frequency signals required for broadband communication [5]. Also, residential loads such as dimmers, switching power supplies, and other communication media often contribute noise in ranges anywhere between 100Hz and 1MHz [6]. Depending on what loads are connected to the line, the line characteristics of impedance, noise, and signal attenuation vary over a wide range and are highly complex and non-linear.

Another problem for PLC is bandwidth limitations due to *regulation*. In most countries, transmissions on the commercial power line are allocated to the range between 3Hz and about 500kHz. For instance, the Federal Communications Commission (FCC) in the United States allows power line transmissions in the 10 – 450kHz range, while European authority CENELEC currently allows for transmissions in the 3 – 148.5kHz range [8][9]. Communication above these ranges is shared by many other operations,

including AM radio and amateur broadcasters [10]. The current bit transmission rate for PLC is severely limited due to these restrictions and regulations.

The most common in-home PLC applications are adjusting lights, turning electronics on and off, and low-speed Internet use. For these purposes, delays on the order of hundreds of milliseconds are tolerable. Thus, such delays are permitted by the technology. Of course, for servo control, this is the same order of magnitude as motor time constants, and is completely unacceptable. Thus, traditional PLC has numerous difficulties that have limited its success so far.

In this research, an alternative architecture will be developed for vast d.o.f. robotic, electromechanical, and vehicular systems. Instead of using an AC power line, signals are transmitted over a DC power bus connecting a DC power supply to various nodes including actuators and sensors. Use of a DC power bus allows us to resolve many difficulties of AC PLC. Furthermore, this DC power bus communication along with proper modem design allows us to connect an order-of-magnitude larger number of actuators and sensors. In the following sections, a new PLC architecture is introduced, its feasibility and noise characteristics are addressed, an effective modem is then designed for broadcasting signals to numerous nodes, and a prototype system is built and tested.

1. DC POWERLINE COMMUNICATION NETWORK

1.1. DC Powerline Communication: Premise

Power line communication (PLC) is a technology used for sending data using pre-existing power lines. PLC allows us to reduce cable requirements, and has been shown to be a useful and economically viable technology in recent years [4][5]. The bulk of PLC research to this point has been done with regards to in-home networks. Current PLC techniques allow signal speeds of up to 1kbps and are expect to reach up to 1 Mbps, and cover communication methods such as phase-locked loop, spread spectrum, and digital modulation techniques [2][5][7]. However, there are a number of limitations to PLC. The large power transformers that are used to step down power from outdoor power lines to individual houses attenuate high frequency signals required to send reliable information [5]. Also, residential loads such as dimmers, switching power supplies, and other communication media often contribute noise in ranges anywhere between 100 Hz and 1 MHz [2]. Depending on what loads are connected to the line, the line characteristics of impedance, noise, and signal attenuation vary in a wide range and are highly complex and non-linear.

Another problem for PLC is bandwidth limitations. In most countries, transmissions on the commercial power line are allocated to the range between *3 Hz* and about *500 kHz*. For instance, the FCC in the United States allows power line transmissions in the *10 – 450 kHz* range, while European authority CENELEC currently allows for transmissions in the *3 – 148.5 kHz* range [8][9]. Communication above these ranges is shared by many other operations, including AM radio and amateur broadcasters [10]. Therefore, the current bit transmission rate for PLC is severely limited due to these restrictions and regulations.

1.2. Architecture

Our powerline communication architecture is intended to apply to a confined, local system where DC power is supplied to all the nodes connected to the system. Such a closed environment with a shared DC power supply can be found in robotic systems, vehicles, and manufacturing equipment, many of which contain a number of actuators and sensors to be connected. As shown in Figure 1, a single power bus line originating in a DC power supply extends to a number of nodes (in this case, 'nodes' refers to actuator and sensor units). Data to be transmitted, such as encoder readings, sensor signals, and control commands, are coded, modulated, and sent over the DC power bus by superimposing high frequency signals on top of the DC power supply voltage. Each node is equipped with a modem for superimposing and tapping the signal as well as coding and modulating the signal. With this DC powerline communication, cable requirements will significantly be reduced in robotic and vehicle systems and elsewhere. A single line, carrying DC voltage and data signals, that we term the Consolidated Power/Signal (CPS) line, and a ground line are needed to connect all the nodes.

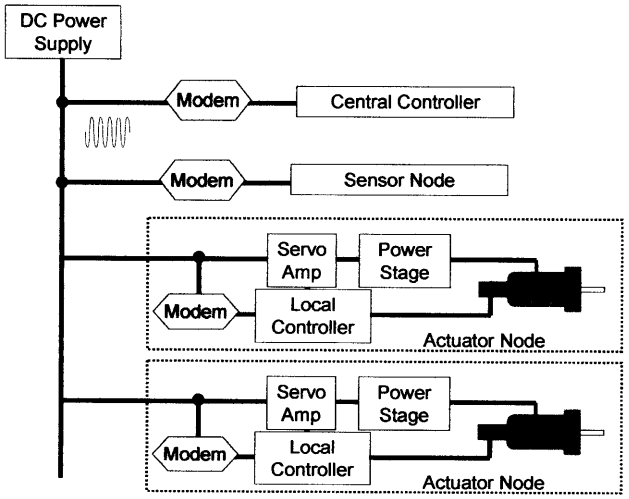

Fig. 1. Architecture of DC power bus communication system

This powerline communication architecture has the potential to apply to a broad range of electromechanical systems having distributed servo drives and sensor drives. Note that, unlike traditional layouts of actuator drive systems, where drive amplifiers are placed inside a control console and long cables are used for connecting the actuators to the drives, this DC power bus network entails distributed drives placed near the actuators. As shown in Figure 1, a servo amplifier and a power stage together with a local controller are placed near the actuator, leaving a long distance power and data transmission to the single CPS line. Since the cables between the actuator and the drive are in general high voltage, high *dV/dt* lines, reducing the distance of such cables will effectively reduce electromagnetic interference (EMI) and ground noise. The proposed DC power bus network capitalizes on this feature of distributed drive amplifiers[1].

This DC power bus communication has a few more important features. The DC power supply acts as a buffer between the DC bus line and loads on the AC mains. Because of this, the line's characteristics do not depend on those loads beyond the DC power supply. Furthermore, since no large transformers (which act as large inductances) are directly connected to the line, the line impedance at high frequencies is much higher than that of the traditional AC power line. Another important advantage of DC power bus communication is that the load conditions are known or at least predictable, since the power bus line is connected only to a known set of nodes that can be quantified prior to operation. Modems for transmitting signals can be designed based on the known characteristics of loads and noise sources. This allows for the reliable broadband communication needed for multi-axis servo control.

[1] So-called integrated motors and smart motors have their servo amplifiers housed inside the actuator body. In the proposed system, the servo amplifier does not have to be inside the actuator body, but can be placed anywhere between the actuator and a DC power supply.

1.3. Technical Issues

The previously described architecture may have numerous variations and diverse levels of sophistication. In this research, however, a focus will be placed on the basic physical layer and hardware modem design suitable for DC powerline communication. In designing such a physical layer an immediate concern of the technology is whether or not the DC bus can be used as a communication medium. Interference with the DC power supply might make the powerline communication infeasible or difficult. There are two possible failure scenarios that must be considered. The first is severe attenuation of the data signal. There is a possibility that the low impedance of the DC power supply will draw too much signal current and substantially attenuate the data signal. Additionally, most DC power supplies have active regulators, which act to minimize ripple in output voltage or current. These regulators might also attenuate the data signal. The second possible failure scenario is due to the fact that many power supplies and converters have switching components. This switching is noisy and may corrupt the data signal.

We must ensure that these adverse effects of using the DC bus can be substantially neglected over the frequency ranges in which we hope to transmit data.

1.3.1. Attenuation due to DC Power Supply

Much work has been done to characterize the AC powerline [4][5], which is fundamentally different from the DC powerline. So far, little data is available on DC powerline characteristics. For this research, linear switching power supplies and fixed voltage power supplies are considered. All DC power supplies are modeled simply as an ideal voltage/current source in series with a small impedance. In actuality, linear power supplies have capacitors, resistors, inductors, and other discrete components at the output

terminals for regulation purposes. Due to these components, DC power lines exhibit frequency-dependent impedance characteristics as shown in Figure 2.

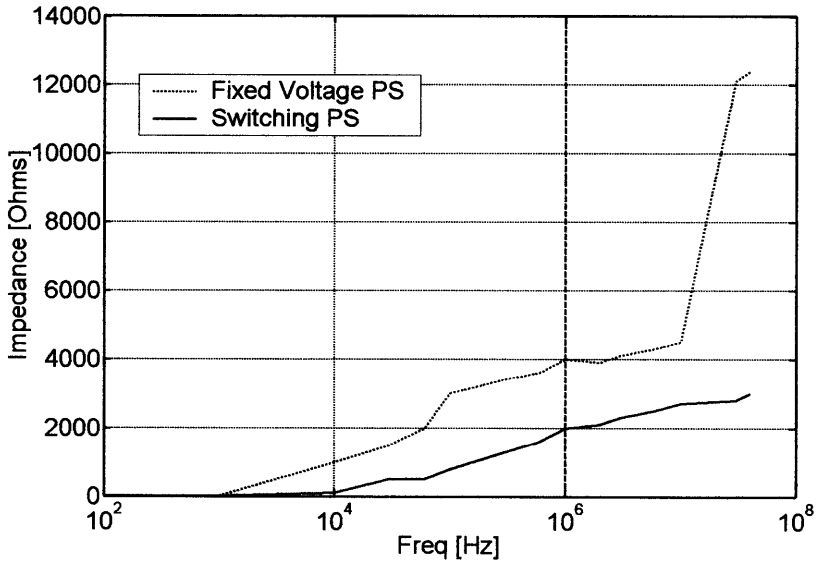

Fig. 2. Impedance measured for fixed-voltage and linear power supplies

Figure 2 shows results from experiments of output impedance measurements of a passive fixed-voltage power supply and an active switching power supply. Note that, at frequencies above 100kHz (the dashed line of Figure 2), the DC power supply terminals have very high impedance. This is due to the high frequency impedance of the power supply output inductance. Additionally, the control circuit cannot regulate the output line voltage quickly enough to attenuate the signal.

This high impedance implies that at high frequencies, even a little signal current may not flow into the DC power supply. Thus, attenuation due to the power supply at high frequencies is limited and quantifiable. The results are encouraging, since they allow for high frequency transmission, which corresponds to higher transmission bandwidth. As long as the carrier frequency of the transmitted signal is above a certain threshold, the DC bus line has the potential to be used as an effective communication media.

1.3.2. Noise Corruption

Both a fixed voltage and linear switching power supply have been tested experimentally to examine noise characteristics. Figure 3 shows noise measurements of noise levels in the power supplies. The fixed voltage power supply showed that the largest amplitude noise was –50dBv at 60Hz, well below ideal transmission frequencies. This noise is due to switching at the AC mains frequency. The linear switching power supply showed higher frequency noise characteristics. The noise from the switching power supply had maximum amplitude of –50dBv at 380kHz.

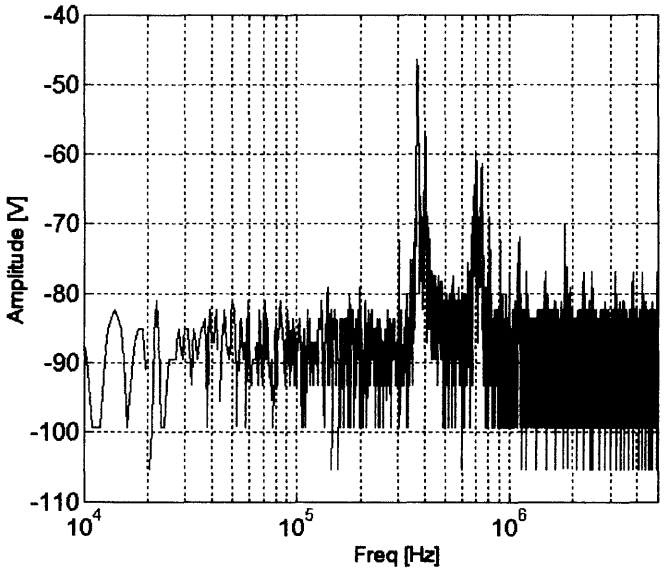

Fig. 3. Noise in linear switching power supply

The two large noise spikes are due to the voltage rectification that takes place in the power supply. This is in the high frequency range; however, this noise is inherent to the system and does not change with time. Thus, to adequately eliminate these adverse effects, it is necessary to choose transmission frequency ranges that do not coincide with these noise spikes.

2. MODEM DESIGN AND ANALYSIS

2.1. Hardware Requirements and Problems

Given that the DC powerline is feasible to use as a communication medium, we now determine a method for fully exploiting the features of the DC powerline communication. Specifically we are interested in networking a large number of actuators and sensors, as described previously. For such applications requiring vast numbers of nodes, the fanout of the modem must be large. Signals must not attenuate significantly although many nodes are connected to the CPS line. Furthermore, the line impedance must remain high enough to keep the driving current low even when large numbers of nodes are connected to the CPS line. To meet these goals, an efficient modem design will be presented in this section. The modem must facilitate reliable communication between the sender side components and the receivers.

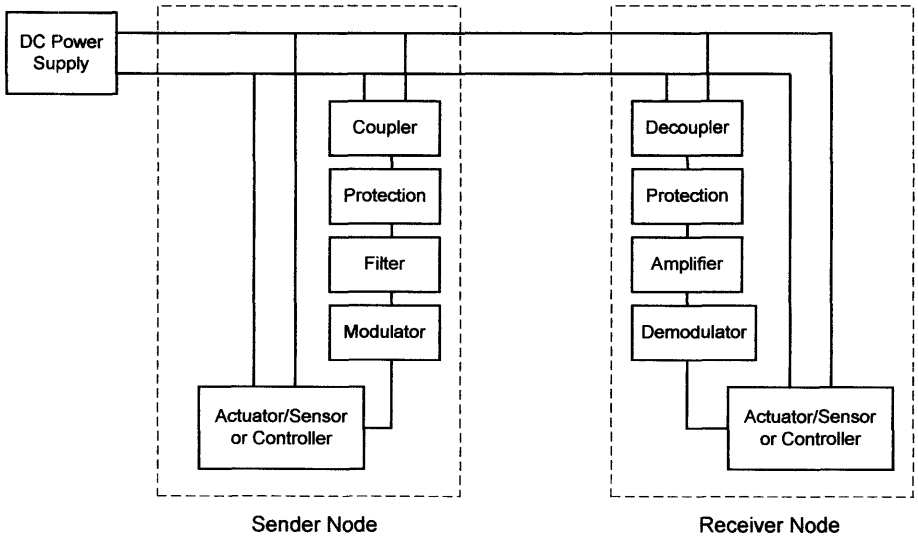

Fig. 4. Block diagram of DC Bus transmission components

Figure 4 illustrates the major components required for sender and receiver nodes. The modulator, demodulator, amplifiers, and filters are all standard modem components.

However, because this modem is for use in a PLC system, additional protection, coupling, and decoupling components are required. The primary functional requirement for these components is the ability to superimpose the data signal onto the DC power line. Additionally, we must be able to block DC voltage and current to prevent saturation of and damage to the modem. The protection must not, however, impede the combination (and separation) of the data and power by the coupler (and decoupler). The components must also maximize signal power deliver to the receivers and have a minimum insertion loss. Finally, we wish to be able to communicate with a large number of nodes, despite the fact that they are paralleled on the bus line.

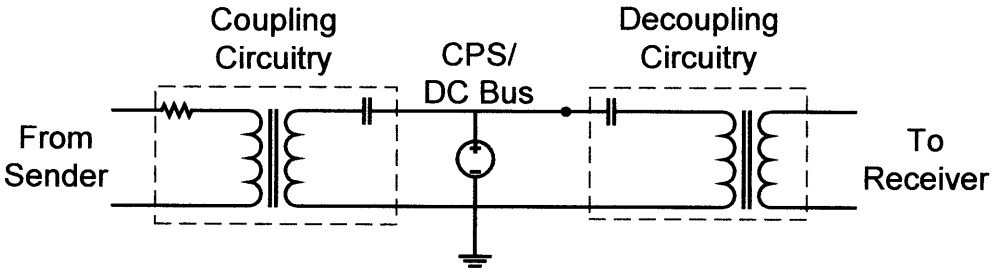

Fig. 5. Standard coupling/decoupling circuitry

Figure 5 depicts a standard coupling and decoupling circuit used for AC powerline communication. The transformer electrically isolates the data and power sources. The capacitor is used to block DC power from the modem transmit and receive components. The transformer and capacitor provide a path for the AC data signal to be superimposed on the DC powerline. This type of coupler and decoupler is commonly used in current PLC technology [11]. This standard circuit, however, does not meet our requirements due to the parasitic effects of the transformer at high frequencies. Parasitics such as winding resistance and magnetizing inductance are ignored in the ideal transformer model. These parasitic effects cannot be neglected for high frequency applications such as ours. Many

of the parasitics actually show up in parallel with the transformer windings. At high frequencies, these parasitics cause resonances that detract from ideal behavior and draw non-negligible amounts of current, termed insertion losses. This current flows from the supply line directly to ground, and never passes to the load. Thus, there can be substantial attenuation of the data signal. As the number of nodes increases, this attenuation can critically reduce the data signal level on the CPS until it is too low to drive the receiver nodes.

2.2. Use of Transmission Line Transformer

To minimize the insertion losses associated with the coupling and decoupling circuits, we propose to apply the theory of transmission line transformers (TLTs). The basic building block of the TLT, shown in Figure 6, transmits energy to the load by use of transverse transmission line mode. Depending on the grounding and the connection of the terminals (terminals are marked 1 through 4), different functionalities result. Placing a load across terminals 2 and 4, and varying the grounded point can produce a phase inverter or delay line, for example. It is known that transmission line transformers have substantially lower insertion losses than traditional transformers for various applications [12][13]. Details of the functionality of the TLT in telephony are explained in Appendix 6.3.

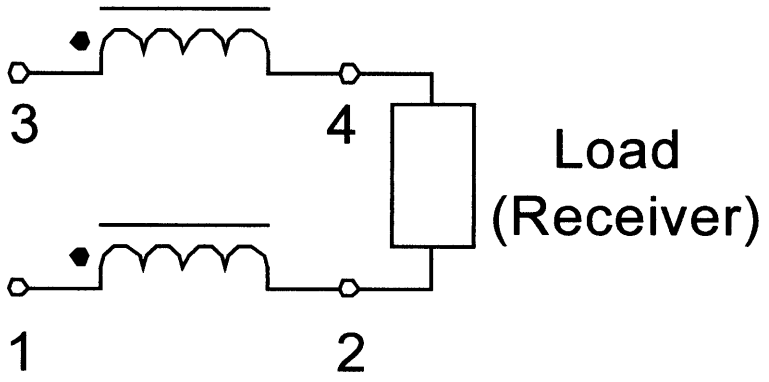

Fig. 6. Basic building block for transverse transmission mode circuits

A major advantage of TLTs is that the parasitics associated with the transformer, many of which show up in parallel with the windings, are now in series with the load. Thus, even when these parasitics draw non-negligible current at high frequencies, the current is ultimately delivered to the load. As stated, a standard transformer allows this current to flow directly to ground, bypassing the load. Thus, the TLT is less susceptible to losses due to parasitic effects.

To our knowledge, no one has ever used TLT's for power line communication. In this research we design a high fanout modem by exploiting these features of the TLT. To do so, we must ensure that the signal current flows to the modem components at the receiver side, and not into the power supply. A class of TLT configurations termed Guanella TLTs meets this requirement since it transforms the impedance. Namely, this can make the power supply impedance, $Z_{ps}(jw)$, look much higher than that of the receivers, $Z_r(jw)$. The overall modem design, including the Guanella TLT, is shown in Figure 7. This Guanella TLT performs a 1-to-4 impedance transformation. This ratio of impedance transformation can be changed with additional Guanella TLTs. As we will show later, however, a ratio of 1:4 is adequate for our application.

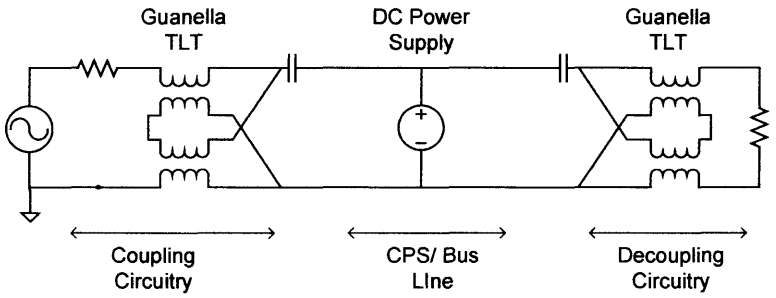

Fig. 7. Coupling and decoupling circuits with transmission line transformer

The design of this Guanella TLT is governed by the behavior of its parasitics. The parasitics of the transformer can be tuned by careful design. By tuning the parasitics along with the DC blocking capacitor, we can match the sender and receiver impedance to maximize power delivery and suppress reflection. To analyze the desired component values, it is critical to understand the operation of the TLT.

2.3. TLT Modeling

We start by analyzing the frequency characteristics of a single TLT and build a lumped parameter model competent to depict parasitic dynamics in a relevant frequency range. The TLT is uniquely designed for each application, so there is no standard model. We must assume a model and verify it with experimental results. The model we used is based on that presented by Kuo [13]. Traditional TLT models are accurate only over limited frequency ranges. Often separate models are required to predict the operation of a TLT over a wide frequency range (up to mega-Hertz). However, Kuo's model can predict both the low and high frequency responses of the TLT. This model incorporates the magnetizing inductance and winding resistance of the transformer in parallel with the TLT windings. The difference in our formulation is due to the fact that a basic 1:1 isolating transformer is modeled by Kuo [13], whereas a 1:4 Guanella style transformer is

needed in this research. Nonetheless, the applicability of Kuo's model to our Guanella TLT is verified by close agreement between experimental and model results. Based on this model, the ideal TLT circuit of Figure 7 is redrawn in Figure 8 to explicitly include the parasitic dynamics magnetizing inductance, L_m, and winding resistance R_o.

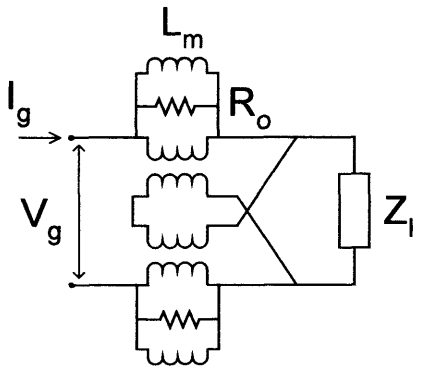

Fig. 8. Guanella transmission line transformer model accounting for magnetizing inductance and winding resistance

Let I_g and V_g be the Guanella input current and voltage, respectively, and $Z_l(jw)$ the equivalent load resistance placed across the output terminals. TLT impedance $Z_l(jw)$ seen at the input terminals is given by:

$$Z_l(j\omega) = \frac{V_g(j\omega)}{I_g(j\omega)} = \left(\frac{8R_oZ_l}{Z_l + 2R_o}\right) \frac{j\omega}{j\omega + \left[\frac{2}{L_m}\left(\frac{R_oZ_l}{Z_l + 2R_o}\right)\right]} \tag{1}$$

We first experimentally determine the values for L_m and R_o. Impedance data was collected with an HP4194A impedance analyzer with bandwidth of 40MHz. The TLT was terminated with various resistors, and the impedance of the TLT/resistor combination was measured. The experimental values for the parasitic components were plugged into the impedance function (1) to obtain a numerical solution. The magnetizing inductance was found to be 5μH, and the winding resistance is 450Ω. These values were used along with various resistive terminations to produce the following figure, comparing the

experimental and model results. Note that, in Figure 9, there is close correlation between the experimental and model performance for the load resistance values of 50Ω, 100Ω, and 200Ω.

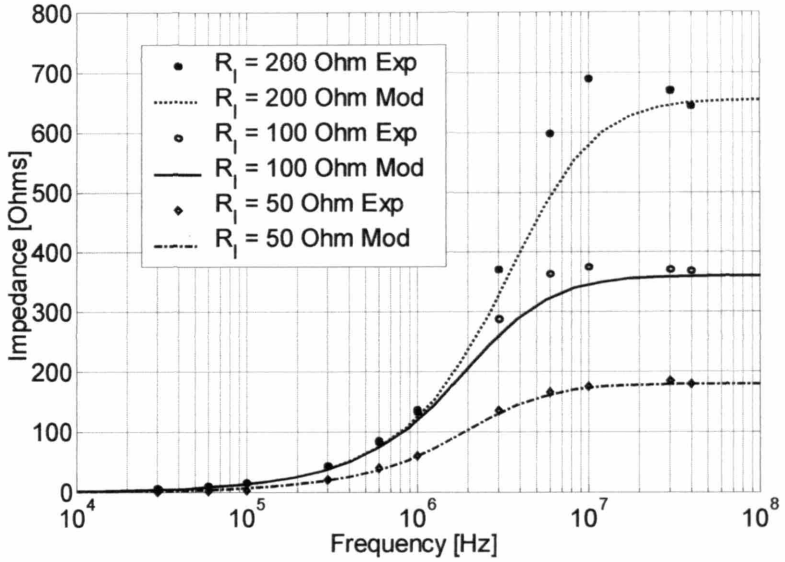

Fig. 9. Impedance of transmission line transformer with terminating resistor

2.4. System Performance

Having verified the TLT model, the next step is to evaluate the system performance when a number of nodes are connected to the CPS line through the Guanella TLT (See Figure 10). Note that the Guanella TLT is arranged in symmetric form for the sender and the receivers. Specifically, we are interested in broadcasting data to many receiver nodes, as illustrated in the figure. Gain and impedance must be evaluated as the number of nodes n becomes large. The impedance seen from the sender-side terminals is given by:

$$Z(j\omega) = \frac{V_{in}(j\omega)}{I_{in}(j\omega)} \tag{2}$$

The frequency transfer function from the input voltage of the sender to the output voltage of a receiver is given by:

$$G(j\omega) = \frac{V_{out}(j\omega)}{V_{in}(j\omega)} \tag{3}$$

Note that V_{in} is the sinusoidal voltage input generated by the sender and V_{out} is the voltage observed at one of the receivers at steady state. I_{in} is the sender-side current associated with the voltage V_{in}.

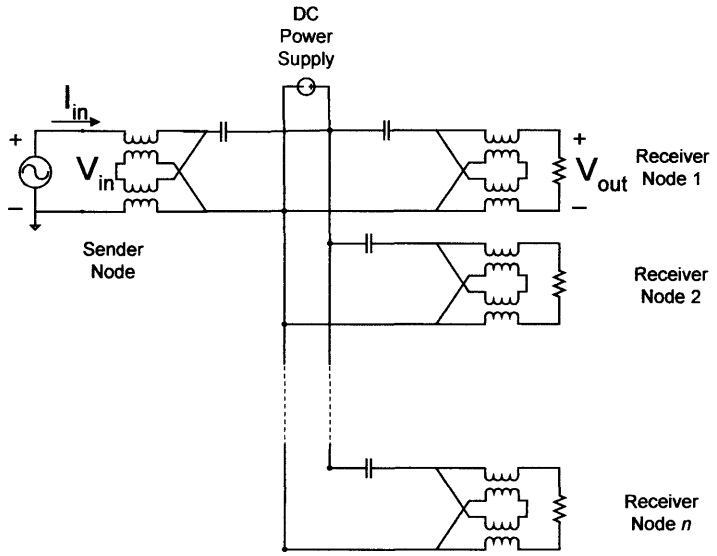

Fig. 10. An *n*-node system with relevant voltages and currents

Analytically, the impedance and gain functions can be found by decomposing the circuit into individual components and using Kirchoff current and voltage laws. These components are shown in Figure 11 (with the DC power supply eliminated for clarity).

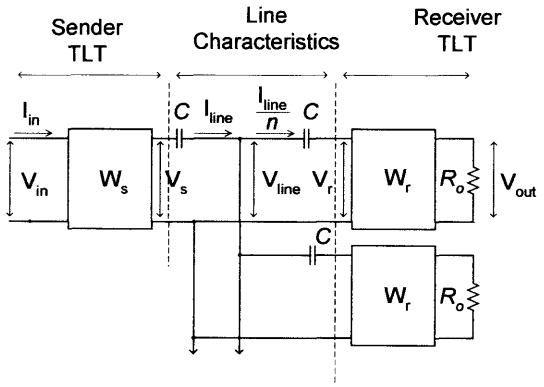

Fig. 11. Circuit divided into sections: sender side components, CPS, receiver side components

To obtain the impedance and gain functions, it is convenient to use a 2x2 matrix formulation relating input current and voltage to output current and voltage. This allows us to evaluate the system characteristics independent of the loads and on a component-by-component basis. As shown in Figure 11 the whole system can be divided into the sender TLT, the receiver TLT, and the line characteristics including the blocking capacitor. Rewriting the impedance of the sender side Guanella TLT given in (1) in 2x2 matrix form, we get;

$$\begin{bmatrix} V_s \\ I_{line} \end{bmatrix} = \begin{bmatrix} & W_s & \end{bmatrix} \begin{bmatrix} V_{in} \\ I_{in} \end{bmatrix} \tag{4}$$

where

$$W_s = \begin{bmatrix} 1/2 & 0 \\ -\left(\dfrac{1}{4R_o} + \dfrac{1}{2L_m s}\right) & 2 \end{bmatrix} \tag{5}$$

Similarly, the impedance of the receiver-side TLT can be rewritten as;

$$\begin{bmatrix} V_{out} \\ I_{out} \end{bmatrix} = \begin{bmatrix} & W_r & \end{bmatrix} \begin{bmatrix} V_r \\ I_{line}/n \end{bmatrix} \tag{6}$$

where

$$W_r = \begin{bmatrix} 2 & 0 \\ -\left(\dfrac{1}{4R_o} + \dfrac{1}{2L_m s}\right) & \dfrac{1}{2} \end{bmatrix} \tag{7}$$

Note that I_{line}/n gives the current flowing to each receiver at steady state. In our target applications, such as robotic systems, the length of the CPS line is at most 10m. The phase shift due to the distributed impedance of the CPS conductor is not significant as long as the carrier frequency of signal transmission is lower than 10 MHz. Assuming that all the blocking capacitors involved in both sender and receivers are the same and that the line impedance is dominated by the blocking capacitance, we can relate the receiver-side voltage and current to those of the sender-side by;

$$\begin{bmatrix} V_r \\ I_{line}/n \end{bmatrix} = \begin{bmatrix} & W_{line} & \end{bmatrix} \begin{bmatrix} V_s \\ I_{line} \end{bmatrix} \tag{8}$$

where

$$W_{line} = \begin{bmatrix} 1 & -\left(1+\frac{1}{n}\right)\frac{1}{Cs} \\ 0 & \frac{1}{n} \end{bmatrix} \tag{9}$$

Combining the above 2x2 matrices, (4),(6), and (8) gives;

$$\begin{bmatrix} V_{out} \\ I_{out} \end{bmatrix} = \begin{bmatrix} W_r \end{bmatrix} \begin{bmatrix} W_{line} \end{bmatrix} \begin{bmatrix} W_s \end{bmatrix} \begin{bmatrix} V_{in} \\ I_{in} \end{bmatrix} \tag{10}$$

Solving this for the impedance V_{in}/I_{in} subject to the load resistance $V_{out}=R_{out}/I_{out}$ yields;

$$Z_n(s) = \frac{As^3 + Bs^2 + Cs}{Ds^3 + Es^2 + Fs + G} \tag{11}$$

(See Appendix 6.1 for coefficients)

As the number of nodes, n, tends to infinity, the impedance function reduces to;

$$Z_\infty(s) = \lim_{n \to \infty} Z_n(s) = \frac{b_1 s^2 + c_1 s}{d_1 s^3 + e_1 s^2 + f_1 s + g_1} \tag{12}$$

These coefficients are dependent on two effective time constants, $\tau_1 = R_o C$ and $\tau_2 = \sqrt{LC}$. Typically, the order of magnitude is hundreds of Ohms for the core resistance whereas the capacitor is in nano-Farad range, and the inductance in micro-Henries. Thus, the time constant τ_1 is on the order 10^{-6} and τ_2 is 10^{-7}. Using these values, we find that $b_1 << c_1$ and $d_1 << e_1, f_1, g_1$. Using the coefficients found in Appendix 6.1, Z_∞ can be further simplified to:

$$Z_{\infty}(s) \cong \frac{c_1 s}{e_1 s^2 + f_1 s + g_1} \tag{13}$$

Similarly, the gain function G(s) for n receivers is given by;

$$G_n(s) = \frac{\alpha s^3}{\delta s^3 + \gamma s^2 + \varsigma s + \varepsilon} \tag{14}$$

(See Appendix 6.2 for coefficients)

As n approaches infinity, the gain function reduces to;

$$G_{\infty}(s) = \lim_{n \to \infty} G_n(s) = 0 \tag{15}$$

This is expected, as the total impedance of an infinite number of paralleled impedances will go to zero. The impedance function $Z_n(s)$ and gain function $G_n(s)$ are plotted in Figure 13 for n=1, 10, 100, and 1000.

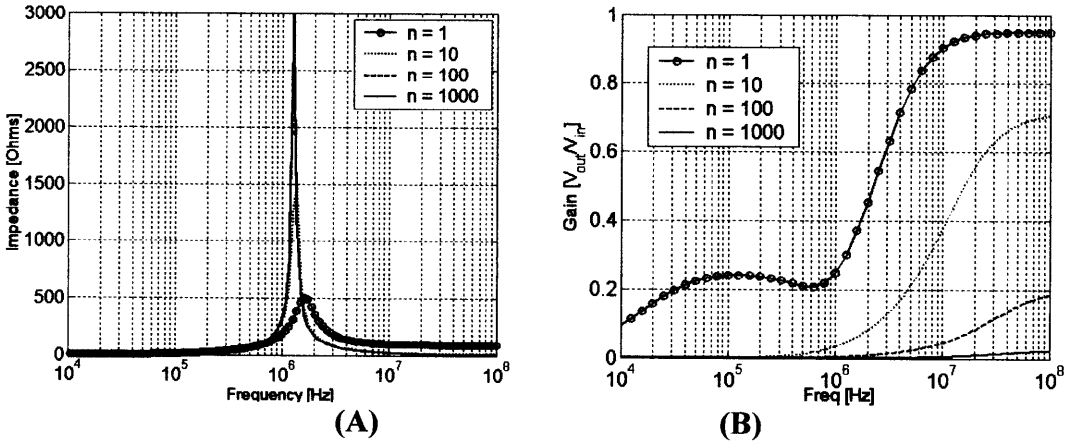

Fig. 12. Impedance and gain as a function of *n*

The plot in Figure 12(A) shows the changes in the impedance characteristic in relation to the number of receivers, n, and frequency. As the number of nodes increases, the magnitude of the peak's impedance increases, peak frequency decreases, and high frequency impedance decreases. It should be noted that, as the number of nodes tends to infinity, the impedance at the peak value becomes extremely high, rather than decreasing.

This large impedance would allow us to broadcast data signals to a vast number of nodes at once. That is, we can choose a point of high impedance so that the sender does not have to provide a large current even though there are numerous loads in parallel. Note that the impedance curve has a peak around 1MHz and that the peak value increases as n increases. This peak frequency can be obtained from (13).

The physical sense of this peaking behavior can be explained with Figure 13. The experimental result can be used to gain physical insight. Recall that the impedance is of the form (11). As n approaches infinity, it reduces to the form of (13). Then, the peak frequency is given by $\sqrt{e_1 / g_1}$. Referring the parameters of $\sqrt{e_1 / g_1}$ from the appendix reveals that the value can be approximated by a constant multiplied by $1/\sqrt{LC}$, where L is the magnetizing inductance, and C is the coupling capacitance. This implies the resonant behavior of a parallel LC circuit. This is justified by looking again at the circuit. As more loads are placed in parallel, the equivalent load impedance of the paralleled loads approaches zero.

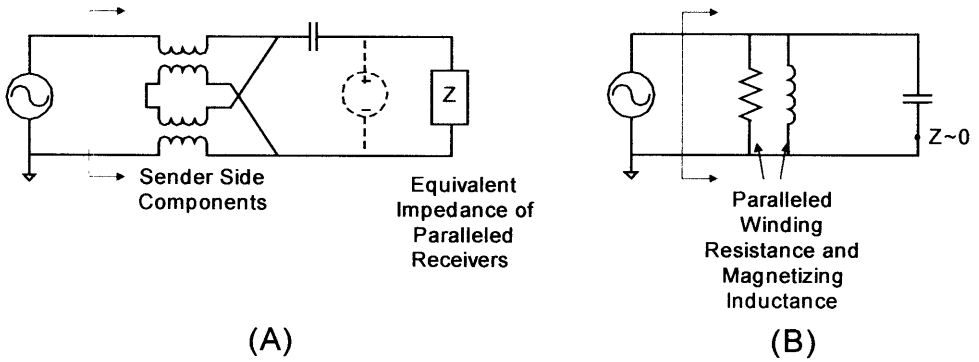

Fig. 13. Equivalent circuit model for large *n*

This effectively changes the PLC equivalent circuit to that of Figure 13(B). The coupling capacitor is in parallel with the winding resistance and magnetizing inductance of the TLT. The impedance function of this parallel RLC circuit matches the form of the

impedance function $Z_{\infty}(s)$. In the equivalent *RLC* circuit, current must always pass through the receiver impedance as well as the sender capacitor. Thus, the use of the TLT ensures that current will always flow into the load. Note that the typical transformer orientation of Figure 5 allows the current to flow right back to the source without passing through the load. Thanks to the TLT, we are able to manipulate the impedance values even for large gain and large numbers of actuators n.

This implies that the proposed modem design using a TLT would allow us to transmit signals to a large number of nodes simultaneously without lowering the output impedance. Refer again to Figure 12(A). Even for large values of n, there remains a regime over which the impedance is high. Due to the TLT, this peak will always remain in the impedance curve. This implies that for any value of n, there will be a high impedance regime. Typically, when fanout becomes large, the impedance goes to zero, and infinite current is required to drive the system. However, in our apparatus, when fanout becomes large, there is always a frequency range for which only a nominal amount of current is required to drive the system. Of course, this frequency range is only useful if the gain of the transfer function, $G(jw)$, is not too small. Therefore, we must examine the gain in the frequency range where the impedance remains high. Specifically, to use this high impedance value, we must ensure that the dip in the gain curve in Figure 12(B) is separable from the peak in the impedance curve by using the design parameters involved in the TLT modem.

In Figure 14, the value of magnetizing inductance was changed from 0.5μH to 5μH to 50μH. In the impedance plot, the peak value changes from 2MHz to 1.5Mz to 850kHz. However, the dip in the gain curve changes from 1.5MHz to 900kHz to 800kHz. Clearly,

the two are not directly linked. Therefore, the gain dip frequency and the peak impedance frequency can be separated.

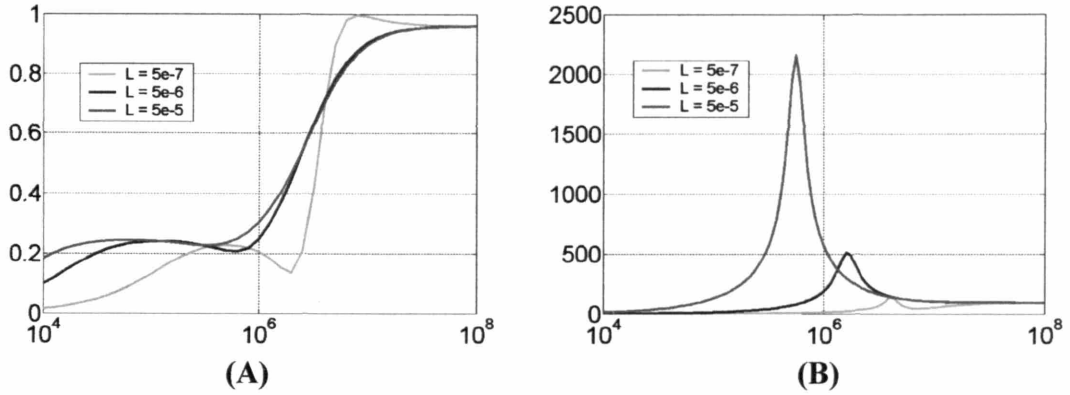

Fig. 14. Characteristic gain dip and impedance peaks for system seen from sender side

Thus, tuning the TLT components also gives us the ability to separate the impedance peak and gain dip, and as a result, allows us to use the high-fanout design protocol. This unique contribution, based on the use of the TLT, allows us to broadcast information to multiple receivers.

3. IMPLEMENTATION AND EXPERIMENTATION

3.1. DC PLC System Prototype

A proof-of-concept prototype system has been developed to demonstrate the proposed approach and verify the design and analysis methods. The prototype has been built in the specific context of developing a large degree-of-freedom robotic system. The goal is to connect all the actuators and their drives and controls with a single DC power bus line. Figure 15 shows the prototype DC powerline communication system connecting 30 actuator nodes located at five separate branches of the CPS line. The system layout mimics that of a humanoid robot. The CPS line originates at the central controller and branches out to the four extremities (two arms and two legs) as well as to a central point within the humanoid apparatus. The total length of the CPS line is 1.83m from the power supply to the most extreme receivers. For the CPS line, a co-axial cable of 75Ω line impedance was used. Six nodes of integrated motors are connected along each extremity, and local feedback controls are installed at the individual motors. The DC power supply is a switching 12V DC regulator. The data transmission rate is 100kbs, which is adequate for transmitting 16-bit reference position data to all 30 local controllers of the integrated motors every 5ms.

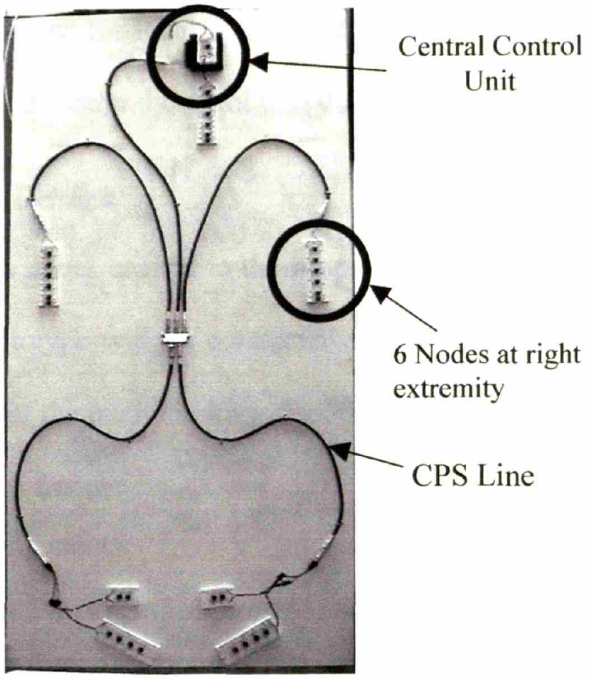

Fig. 15. Prototype DC powerline communication system with 30 nodes

Figure 16 shows the modem used to interface each node with the system.

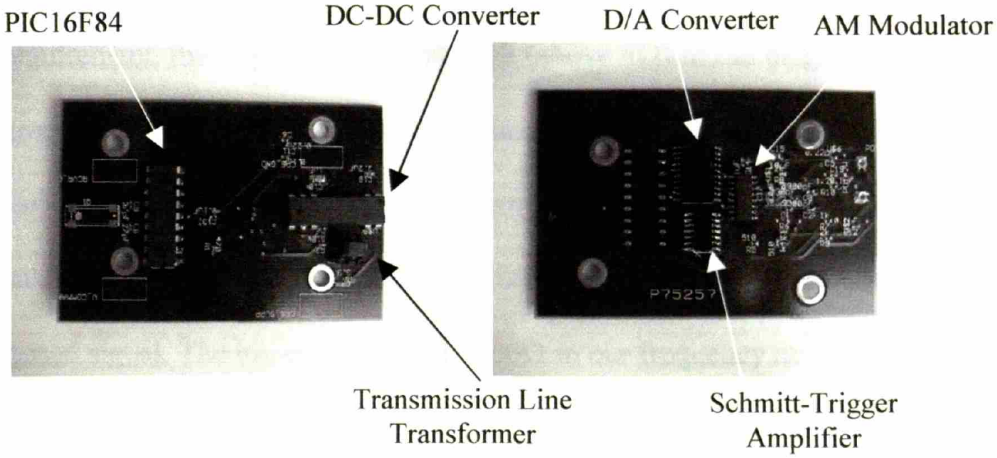

Fig. 16. Top and bottom views of prototype modem

It consists of a transmission line transformer, a coupling capacitor, a microprocessor (PIC16F84), a signal modulation chipset, and a DC/DC converter. A DC servomotor equipped with a 12V PWM amplifier was connected to each node. The microprocessor is

capable of performing computations for local feedback control of the DC servomotor as well as for communication with the central control unit through the CPS line.

3.2. DC PLC System Design

In this section a few design issues critical to the proposed method will be addressed, and experiments using the prototype will be conducted to verify the theoretical results and demonstrate the feasibility of the method. Important design issues include:

- Selection of transmission frequency
- Selection of modem components.

3.2.1. Measurement of Power Supply and Motor Characteristics

We begin with experiments using the motor drives and power supply for quantifying the impedance and noise characteristics. A switching-type power supply was chosen for the DC source. The impedance characteristics measured using an HP4194A impedance analyzer with appropriate protection circuitry has been presented in Figure 2. Per our system requirement, the impedance is very high (above 4Ω) in the mega-Hertz frequency range. However, many motors and drives connected to the CPS line in addition to the power supply. Therefore, the total line impedance including the motors and drives must be evaluated. Figure 17 shows the motor-drive impedance versus the frequency of a superimposed signal. The impedance is over 700Ω in our frequency range of interest.

The noise spectrum was measured with an oscilloscope with a sampling rate of 200 giga-samples/s. The noise spectrum of the power supply has been presented in Figure 3. There are two peaks in the noise spectrum, approximately 380kHz and the 700- to 800kHz range. The noise magnitude is less than –80dBV in the frequency range above 1MHz. Therefore, the carrier frequency should be higher than 1MHz. Figure 18 shows the noise spectrum of the CPS line (with motors and drives connected) when 10 motors

were switched on and off randomly. The noise magnitude remains lower than -43dBV in the mega-Hertz range. However, the noise spikes are large in the hundreds of kilo-Hertz range. For this reason, a low pass filter was inserted across the CPS lines with a sufficiently low cutoff frequency.

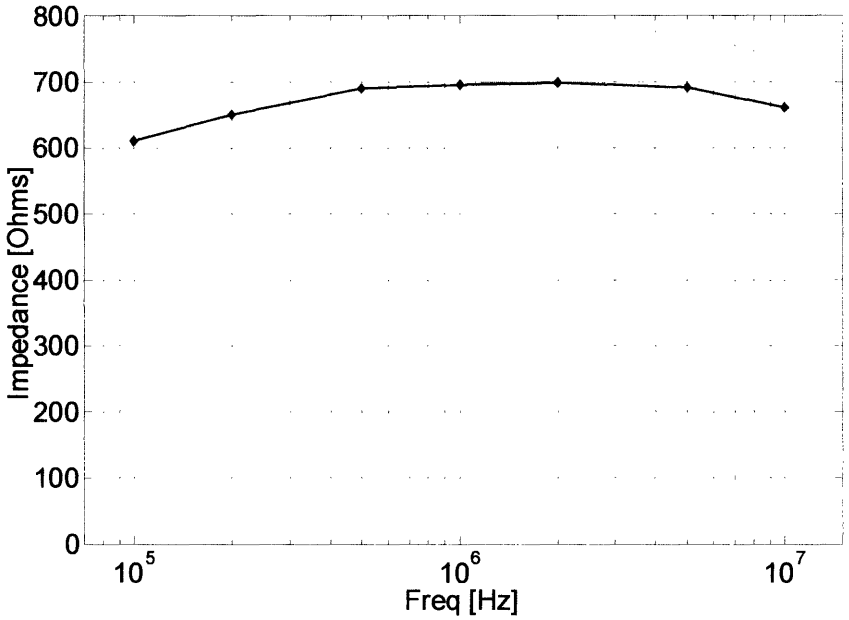

Fig. 17. Motor and driver impedance against frequency

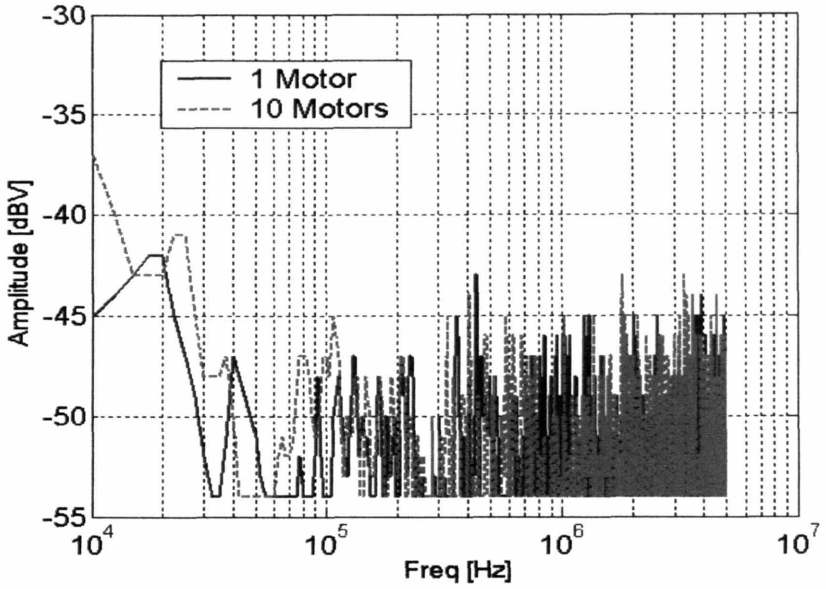

Fig. 18. Noise spectrum of operating motor and noise induced by randomly turning the motors on and off

The desired transmission frequency depends not only on the line impedance and noise characteristics described above but also on the required transmission rate and the gain and peak impedance conditions discussed in the previous sections. Sending command information at and above 100 kbps determines the carrier frequency for modulation. Frequency shift keying (FSK) modulation chipsets using carrier frequencies between 3 and 10 MHz meet this requirement. The required amplitude modulation (AM) carrier frequency is on the order of mega-Hertz[2]. The exact carrier frequency was determined based on the modem's coupling circuit design.

3.2.2. Selection of Coupling Circuit Component Values

We design the coupling circuitry based on the analysis described in the previous section. In turn, experimental data is recorded and compared to the model to verify the design procedure. In addition to the bandwidth restrictions imposed by the power supply

[2] Carrier frequency values of AM chip sets have much more variability than their FSK counterparts. We chose to use AM in order to evaluate the transmission characteristics for a range of carrier frequencies from 2 – 10 MHz.

and motors, filtering and impedance matching conditions determine the values of the coupling circuit component. The design parameters are the transmission carrier frequency f, the coupling capacitance C, and the receiver load impedance $Z_l(jw)$. In addition, we have the TLT impedance $Z_{tlt}(jw)$, its magnetizing inductance L_m, and parallel resistance R_o. The design procedure is as follows.

To determine the TLT parameters L_m and R_o, we first notice that the TLT has high pass filter characteristics. The cutoff frequency is a function of these two parameters and should be tuned such that only transmission frequencies and higher (i.e. the mega-Hertz range as mentioned int he previous section) can pass to the CPS. Thus, the frequency f is found based on the desired transmission rate. We see, from Figure 9, that regardless of load impedance, there is a certain frequency below which no frequencies can pass. This can be used to select R_o and L_m. Having determined L_m and R_o, the next step is to determine $Z_l(jw)$ by evaluating the operating current and voltage for the signal processing components.

The first step after receiving the signal is to demodulate it. At the demodulator, the signal is divided between two ports that can sink a total of 250mA. The input voltage limit is 5V, which gives a minimum input impedance of 20Ω. This is the value used for $Z_l(jw)$. Having found $Z_l(jw)$, we can next find the value for C. The total receiver impedance $Z_{tlt}(jw)$ is the TLT impedance of (1) added to the impedance of the coupling capacitance, $1/Cjw$. For transmission line impedance matching, the impedance of the line must be matched to the impedance of the load to ensure maximum power delivery. Thus, $Z_{tlt}(jw)$ is equal to the impedance of the chosen communication medium (75Ω, in our

case). Setting $Z_{tlt}(jw)$ equal to 75Ω, the only unknown is the capacitance value C. Using this method, all of the values in our system were specified, and are presented in Table 1.

Table 1 Coupling circuit parameter values

Parameter	Value
C	*3.9 nF*
L_m	*5.1 μH*
R_o	*450 Ω*

3.3. Experimental Evaluation

Using the coupling circuit with the aforementioned parameter values and the whole prototype apparatus with 30 actuator nodes, experiments were conducted to demonstrate the feasibility of the design method. Figure 19 shows a source digital signal before modulation and transmission (A), and the demodulated signal received by one of the nodes connected to the CPS lines (B). Here, the pulse interval is 10μs, and the transmission rate is 100kbps. Although the high frequency noise of the power supply is visible in the received signal, the data is correctly decoded. The signal is attenuated by 50%. This confirms our predicted value of gain depicted in Figure 12(B). Although 30 nodes were connected, the signal gain remained high. The signal-to-noise ratio of the received signal was 8:1.

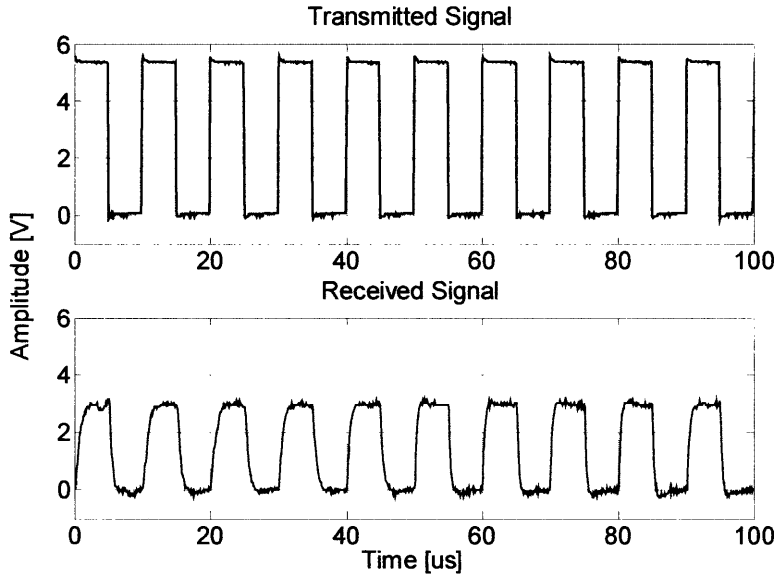

Fig. 19. Original transmitted digital signal and received signal

The key technical feature of the proposed method is to exploit the peak signal transmission impedance that is created through careful selection of coupling circuit parameters and the carrier frequency, as analyzed in the previous section. Using those parameter values determined based on the above design procedure, we can evaluate quantitatively the expression (11), i.e. the signal transmission impedance characteristics viewed from the sender. We can compare this result to the experimental data obtained using the impedance analyzer and the experimental apparatus. The comparison of the signal transmission impedance for a single node, $n = 1$ is shown in Figure20. The comparison for the large d.o.f. robot with $n = 30$ is shown in Figure 21. The experimental values are shown with diamonds, and the model with the solid line. Excluding very high frequencies, there is good agreement between the experimental and the model results. The discrepancy at the high frequencies is due to the equivalent series resistance (ESR) of the coupling capacitor; it is found experimentally that a coupling capacitance ESR value above 100Ω is adequate to elucidate the flat, high frequency behavior.

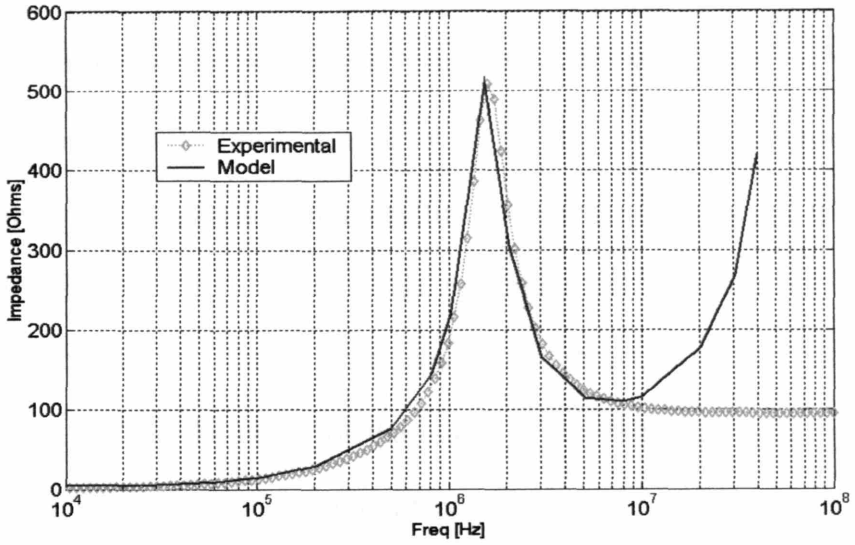

Fig. 20. Signal transmission impedance viewed from sender for $n = 1$

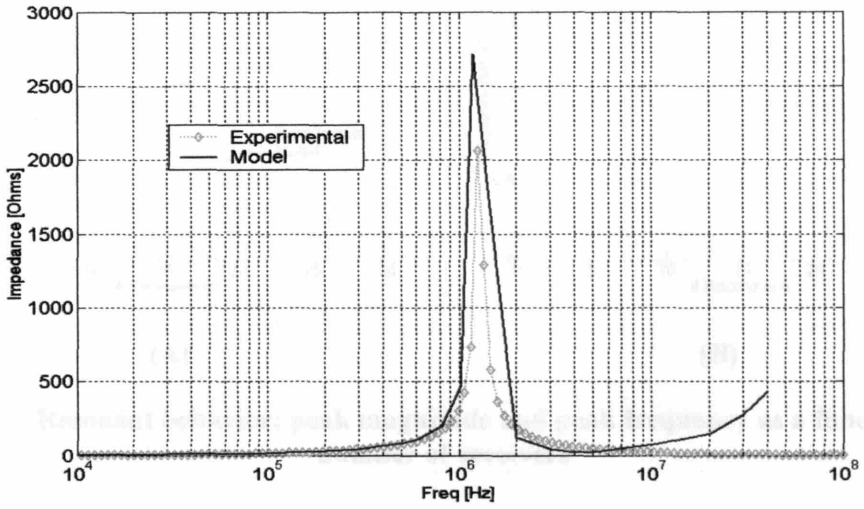

Fig. 21. Signal transmission impedance viewed from sender for $n = 30$

The question may arise as to how well our model predicts the limiting case as n becomes large. To address this issue, it is helpful to look at the model and experimental results as a function of n. Specifically we can look at the magnitude of the impedance peak, and the frequency at which it occurs. We showed earlier that the peak magnitude and frequency reach a maximum and minimum value (respectively) well before n reaches infinity. We now try to calculate the error in the predicted and actual steady-state values.

Figure 22(A) shows how the peak magnitude varies as a function of n according to the model and experimental results. There is 'final' error of 500Ω (20%). For the frequency plot given in Figure 22(B), there is an error of 50 kHz (5%). Thus, while the limiting value of impedance magnitude shows significant error, the frequency at which it occurs can be predicted quite closely. In our design procedure, this frequency is critical because it is used to help determine the parameter values of Table 1. However, the magnitude is not as important. Thus, the utility of the model is verified once again in terms of its ability to predict the limiting behavior as a function of n.

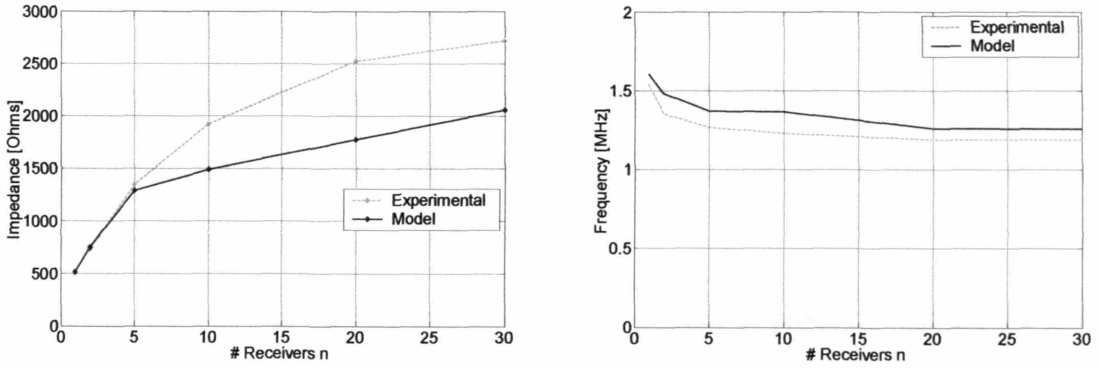

(A) **(B)**

Fig. 22. Resonant behavior; peak magnitude and peak frequency as a function of the number of receivers

4. APPLICATIONS TO HEALTH CARE, HOME AUTOMATION, AND MATERIAL HANDLING

4.1. Health Care and Home Automation

Numerous applications become realizable with the system proposed in this work, including those in the areas of health care and home automation. For example, by reducing all of the power and communication signals to a single cable, the possibilities for flexible machine design are increased. This technology reduces the size of a machine by reducing the required amount of cabling and servo-system components. At the same time, it reduces the machine's weight. Since a single cable is used to connect all of the actuators, it also reduces the machine's complexity. There would be no hanging cables or complicated geometries required to route the cabling. The cabling can be run through the machine structure and shielded from interaction with the user. In this way, the technology allows for much safer designs.

This technology can be very influential in the market of products that aid the elderly, handicapped, and other movement-restricted people. In marketing products to these groups, safety and ease of use are major concerns. By replacing standard systems with the technology presented here, the bulk of any mechanized aid can be limited to the area surrounding the actuators. To better visualize this idea, one can imagine a machine that requires multiple actuators, such as a mechanized walker (Figure 23).

Fig. 23. Mobility aids for disabled children and elderly persons

The mechanized walker and standing aid shown here both use some standard servo-system design. With the apparatus presented in this work, such machines can be simplified. The central controller and power supply (a battery, in this case) can be kept to a small size. Actuators can then be placed directly at the wheels, leaving the rest of the apparatus aesthetically appealing and easily maneuverable. A simple schematic illustrating this idea is pictured in Figure 24.

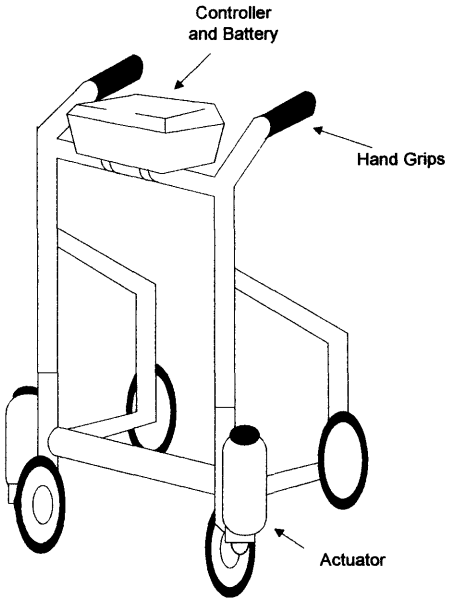

Fig. 24. Automated walker using DC PLC apparatus

One might question the importance of aesthetics. However, consulting a reference such as Human Factors International makes it clear that elderly persons are concerned with the appearance as well as functionality of a product. Oftentimes, a complex or unwieldy-looking machine is very unattractive and perceived as dangerous, and the elderly person simply won't use it. The technology presented here can be used for simple, intuitive looking designs that appeal to all sorts of mobility-impaired users.

4.2. Material Handling

This work also has relevance for material handling systems. Traditionally, such systems are employed in hostile environments (mining shafts), for large, heavy loads of materials (iron works factories), or when only a small amount of material needs to be sent at irregular intervals (bank tellers). There are four common disadvantages of these systems that can be addressed by this work.

Most of these systems require large amounts of space. Large overhead cranes require extensive I-beam structures to support their weight. Belts, and other types of conveyors, need stationary supports that often require the factory to be designed around them. Large apron feeders need space not only for the transport mechanism, but also for the mechanism that places the materials on the feeder.

Another major disadvantage is many systems are '2-dimensional.' Systems such as belt conveyors, roller conveyors, chain conveyors, and bucket elevating conveyors work in either a vertical or horizontal plane [16]. This is a problem because transfer from these systems to the third dimension is costly in terms of finances, space, and time.

Most of these systems also have no intelligence. Pneumatic tube package conveyors involve placing a parcel in a tube and using pressure or a vacuum to propel it to its destination [17]. Clearly, once a package is sent, there is no way to change its destination in real-time. Also, the entire path to a receiver must be clear before a package can be sent.

Finally, one of the most obvious drawbacks of all the systems mentioned is that they are not dynamic. Belted systems require multiple packages all going in the same direction, or only have a single crane capable of moving objects one at a time.

In this work, a new method of transferring materials is presented. This method relies on multiple 'smart-carriers' receiving power and information from the track itself. Additionally, many packages can be simultaneously transferred to different destinations. The intelligence of this system allows destinations to be changed in real-time. Furthermore, it allows each package to 'look' at its destination and find the quickest path (shortest distance, least amount of obstructions in path). Simultaneous delivery of power

and information to each package carrier allows for flexibility of design of the tracks linking each end-point. It is fully 3-dimensional, yet unobtrusive enough that it can operate efficiently in a hospital or office building. A possible implementation is shown in Figure 25:

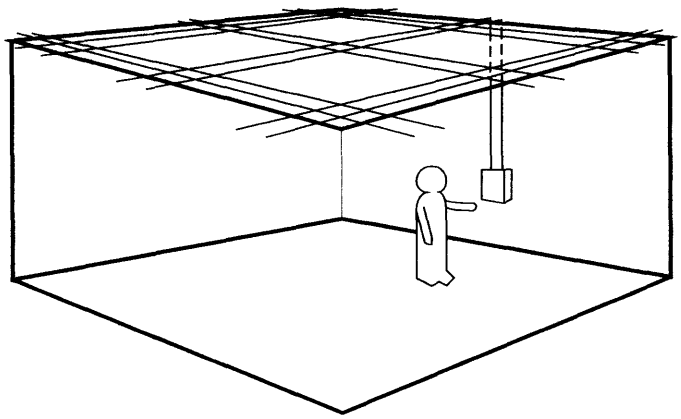

Fig. 25. Office with overhead tracks

This figure shows a system that is mounted on a ceiling, but can still be interacted with on the user's level. We now introduce three salient features of the system.

4.2.1. Power Delivery through Tracks

The architecture we've established for this system allows the power to be delivered to each carrier directly from the tracks (either through sliding or rolling contacts). This eliminates the need for a battery in the carriers, and greatly simplifies the whole system, requiring only a single power supply.

4.2.2. Information Delivery through Tracks

By using a powerline communication network, we are also able to deliver signals to the carriers through the tracks. This guided communication has a number of advantages including low susceptibility to environmental interference. Therefore, when developing a communication standard for the system, adverse environmental noise can be largely ignored. Additionally, in some environments, such as hospitals, radio frequency

communications are not permitted. Therefore we are still able to send information, change carrier destinations, and locate carriers in real-time without interfering with hospital measurement equipment.

4.2.3. 3-Dimensional Travel

As mentioned, the majority of material handling systems move only in a (vertical or horizontal) two-dimensional plane. However, our system is fully three-dimensional. Therefore, the majority of the traffic can take place in a ceiling or between floors, out of the way of normal human activity. At the same time, the endpoints of the track network extend down to the level of the user. Additionally, the track can extend downwards (or upwards) to multiple floors if necessary.

5. CONCLUSION

In this work, we had two goals. The first was to assess the feasibility of using a DC power bus for data communication, and the second was to design a system to take advantage of the unique communication medium.

We started by discussing the specific technical issues specific to the use of a DC source as a data medium. These technical issues are the impedance and noise characteristic of the line, and of all other connected components. We found that, despite the presence of power supply components that act to attenuate the signal, intelligent design of the coupling and decoupling components will allow for favorable impedance and noise characteristics on the CPS.

After having established the feasibility of the DC bus, we next sought to take advantage of the inherent characteristics. To do so, we proposed a DC PLC system that consists of a centralized power supply and controller, and a multitude of 'smart nodes.' The advantages are high variability and a dynamic structure can be applied in numerous areas. We find that transmission line transformers are useful for creating a high fanout, high bandwidth system.

We have created an experimental apparatus to confirm our system model. Further, it has been demonstrated that our design process is useful for communication with multiple nodes connected in parallel to the CPS. This technology can serve as a foundation for advances in numerous areas.

6. APPENDICES

6.1. Impedance Coefficients

$$\alpha = \left(\frac{R}{R+8R_o}\right), \tau_1 = R_oC, \tau_2 = \sqrt{LC}$$

$$A = 16\alpha(R_oC)(LC) = 16\alpha\tau_1\tau_2^{\,2}$$

$$B = 8(n+1)R_o(LC) = 8(n+1)R_o\tau_2^{\,2} = b_1n + b_2$$

$$C = 16\alpha(n+1)R_o(R_oC) = 16\alpha(n+1)R_o(\tau_1) = c_1n + c_2$$

$$D = 2(n+\alpha)(R_oC)(LC) = 2(n+\alpha)\tau_1\tau_2^{\,2} = d_1n + d_2$$

$$E = (n+1)\left[4\alpha(R_oC)^2 + LC\right] = (n+1)\left[4\alpha\alpha_1^{\,2} + \tau_2^{\,2}\right] = e_1n + e_2$$

$$F = 2(1+\alpha)(n+1)(R_oC) = 2(1+\alpha)(n+1)(\tau_1) = f_1n + f_2$$

$$G = 2\alpha(n+1)\frac{(R_oC)^2}{LC} = 2\alpha(n+1)\frac{\tau_1^{\,2}}{\tau_2^{\,2}} = g_1n + g_2$$

6.2. Gain Coefficients

$$\alpha = 32R_o^{\,3}L^2C$$

$$\delta = 4R_o^{\,2}L^2C\left[9nR_s + R_s + 8R_o\right]$$

$$\varepsilon = 2R_oL\left[4(n+1)R_o^{\,2}R_sC + 9R_sL(n+1) + 72R_oL(n+1)\right]$$

$$\xi = 40(n+1)\left(R_o^{\,2}R_sL\right)$$

$$\eta = 8R_sR_o^{\,3}(n+1)$$

6.3. TLT Functionality: Telephony

The hybrid network is an essential component of communication electronics. Often, local communication is carried out on two lines. Long distance communication may be carried out on four. The hybrid functions as the physical transition between two and four wire communication.

The hybrid network consists of five components: transmit wires, receive wires, impedance match network, local wires, and the hybrid transformer. All incoming information from remote locations comes in on the two receive wires, and all information sent to those locations is sent on the two transmit wires. This is the 4-wire side.

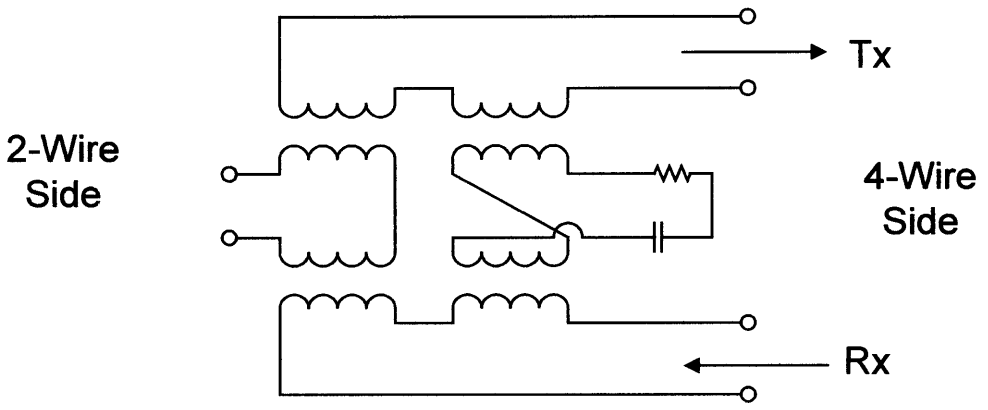

Fig. 26. Hybrid transformer as used in telephony

The impedance matching network is the final requirement for the circuit. This network is tuned to match the characteristics of the local wires. In its simplest form, this network consists of a 600Ω resistor, or a 900Ω resistor in series with a 2.16 μF capacitor. This matching is necessary for the signal cancellation.

Cancellation is required for full-duplex operation. All four components are connected to the hybrid transformer. When a user wants to transmit information from the 2-wire side to a remote location, the signal is split (equally) between the transmit wires and the receive wires. There is current generated in both the *Tx* and *Rx* coils. Thanks to the matching network, the portion of the signal in the receive wires is dissipated as heat so the user does not see a duplicate of his transmitted signal. When a user is receiving information from the 4-wire side, the signal comes through the receive wires, and is split

between the 2-wire side and the match network. Again, the transformer configuration ensures that the current induced in the *Tx* wires is dissipated.

Thus, by use of the hybrid transformer, full duplex communication is achieved. The hybrid is in fact the most critical analog circuit component, as many other components such as filters can be built much more reliably using digital circuitry. This premise can be applied to our situation, but must be *reversed.* Essentially, the 2-wire region of the setup presented in Figure 26 can function as the CPS bus. The fact that there will be DC power across the 2-wire side must be taken into account. The magnetic elements must be designed so that the DC voltage that must be blocked doesn't saturate them.

Coaxial cable is simply a cable with two conductors, one running along the axis and the other separated from it by a concentric insulator. The advantage of coaxial cable is that its inductance, capacitance, and conductance values are mostly independent of frequency. The geometry of the cable reduces radiation and cross talk effects.

The distinction for wireless transmission is that the propagation of information waves is no longer guided. This requires additional components such as antenna. Because the signal is not guided, a signal transmitted through free space will reach the receiver in a number of different ways. Of course, there is point-to-point communication. But there are also waves that reflect off the ground and the earth's atmosphere, depending on the location of transmitter and receiver.

It is important to remember that antennas will create an output voltage whenever it is receiving any electromagnetic signals. However, the level of this voltage is usually so small that some kind of (powered) amplification is necessary for most functions. For

this reason, most receivers (an AM radio, for instance) require a separate power source in order to receive and amplify a signal.

Other techniques for communication are comparable to the two mentioned above. Twisted pair cable for instance is a physical connection, like coax cable, but has much more frequency dependent impedance characteristics. Wave-guides act similar to coax cable, but lack the inner conductor. However, they get their best performance at high frequencies (10s of giga-Hertz). Optical fibers are also a viable communication method.

The most important characteristic of our system is the simultaneous delivery of power and information. The problem can be viewed from two perspectives: optimizing power delivery methods to accommodate information, or optimizing information delivery methods to accommodate power.

In looking at the communications methods listed above, some quick conclusions can be made in regards to the One-Cable Smart Motor Apparatus. In regards to the physical communication media, twisted pair and coax cable are optimal for the task of simultaneous power and information delivery. The physical structure of wave-guides relies on numerous joints and physical irregularities. This makes using them below optimal high frequencies very difficult. Our system, operating only at megahertz, would be very susceptible to problems. Furthermore, by carrying power in the outer conductor, additional insulation and safety measures are needed. Of course, most current fibers with adequate optical capabilities cannot withstand power delivery as well. Power can cause them to burn or alter the mechanical properties that make optical information delivery possible.

Transmitting power through the air is extremely difficult. To transmit and receive signals, communication systems rely on high frequency signals. DC is not transmitted, only small amplitude high frequency signals. The resonance in the receiving antennas completes the transmission path.

Functionally, it is difficult to transmit large amounts of power using free space propagation. However, many motors, such as those found in cars, require a lot of power. Therefore, it is optimal to make use of the resources already there, i.e. physical connections. Using the example of the car, there is already a dedicated physical construct, i.e. the chassis. Ideally, the chassis can function as a common ground for the automobile. An additional 'bus' can be added in the form of a cable, or even another rigid physical link, that is electrically isolated from the chassis. Thus, there is a DC ground and power bus that can be built around the currently existing car structure. This idea can be expanded to most other servo systems as well.

Therefore, I have chosen the approach to look at information delivery and optimize it for power transmission as well.

Appendix References; [18][19][20]

7. REFERENCES

[1] Inside Asimo. {Online]. Available: http://asimo.honda.com/inside_asimo.asp?bhcp=1

[2] Graf, Alfons [Online]. (1996). SIPMOS high-current switches in automotive Electronics: Extra Features Cut System Costs. [Online]. Available: http://www.infineon.com/cmc_upload/migrated_files/document_files/Application_Notes/graf2.pdf

[3] Borrill, P.L. "MicroStandards Special Feature: A Comparison of 32-Bit Buses," *Microprocessors and Microsystems,* Vol. 5, No. 6, Dec. 1985, pp. 94-100.

[4] Hines, David. "Unlocking the Potential of Power Distribution Networks," *Powerline Communications*, April 2000.

[5] Strassberg, Dan. "Powerline Communication: Wireless Technology," *EDN Magazine*, June 1996.

[6] Downey, W. and Sutterlin, P. "Power Line Communication Technology Update," *Echelon Corporation Presentation.*

[7] Tanaka, Masaoki. "High Frequency Noise Power Spectrum, Impedance and Transmission Loss of Power Line in Japan on Intra-building Power Line Communications," IEEE Transactions on Consumer Electronics, Vol. 34, No. 2, May 1998.

[8] Newbury, John E. "Communications Services using the Low Voltage Power Distribution Network," Transmission and Distribution Converence and Exposition, 2001 IEEE/PES, P. 638-640, Vol. 2. Nov. 2001.

[9] Chen, Yi-Fu, and Chieuh, Tzi-Dar. "A 100-Kbps Power-Line Modem for Household Applications," International Symposium on VLSI Technology, Systems, and Applications. June 1999.

[10] FCC Bandwidth Allocation Chart, http://www.ntia.doc.gov/osmhome/allochrt.pdf

[11] Korea Kumho Petrochemical. [Online]. Available: www.kkpc.re.kr/pwergraphy/Fundamental.htm

[12] Sutterlin, Philip H. "Powerline Coupling Network," *U.S. Patent*, Patent Number: 5485040, Jan 1996.

[13] Jerry Sevick, *Transmission Line Transformers, Fourth Edition.* Atlanta, GA: Noble, 1996, pp. 1-1 – 3-15.

[14] Ching Chuan Kuo, Ming Ying Kuo, and Mei Shong Kuo, "Modeling and Analysis of Wideband Power Transmission Line Transformers," *Applied Power Electronics Conference and Exposition,* 1996. APEC '96. Conference Proceedings 1996., Eleventh Annual, volume: 1, 3-7 March 1996. pp. 441 – 446 vol.1.

[15] Bigler, Robert A. and Bigler, Punita P. "Integrated DC Servo Motor and Controller," *U.S. Patent*, Patent Number: 591241, June 1999.

[16] Bolz, Harold A. "Materials Handling Handbook," The Ronald Press Company, New York, NY. 1958.

[17] Mulcahy, David E. "Materials Handling Handbook," McGraw-Hill, New York, NY. 1999.

[18] Patrick D. van der Puije, "Telecommunication Circuit Design,"J. Wiley, New York, NY. 2002.

[19] Cass Lewart, "Modem Handbook for the Communications Professional," Elsevier Science Pub. Co., New York, NY. 1987.

[20] Freeman, Roger L. "Fundamentals of Telecommunications," Wiley, New York, NY. 1999.